

EVIDENCE FOR A MASSIVE, DARK GRAVITATIONAL LENSING OBJECT IN Q2345+007

ROBERT C. DUNCAN

Department of Astronomy and McDonald Observatory, University of Texas, Austin, TX 78712

Received 1991 March 8; accepted 1991 April 29

ABSTRACT

We analyze the narrow absorption line spectra of the double quasar Q2345+007. The observed pattern of Ly α forest absorption lines gives evidence that the quasar is gravitationally lensed, with 4-to-1 odds in favor of lensing.

If Q2345+007 is lensed by an object at $z = 1.49$, as suggested by observations of heavy-element absorption lines, then a low-luminosity lensing mass of $\sim 10^{13} M_{\odot}$ contained within a transverse distance $\sim 40 h_0^{-1}$ kpc is implied. The Ly α cloud diameters at $z \approx 2$ would then be $20 \pm 10 h_0^{-1}$ kpc [$q_0 = 0.5$] or $28.0 \pm 14 h_0^{-1}$ kpc [$q_0 = 0$]. If the quasar is not lensed, then the Ly α clouds are larger by a factor of ~ 6.5 .

We suggest several observational tests which might verify the presence of a massive, dark, lensing object and elucidate its properties.

Subject headings: dark matter — gravitational lenses — quasars

1. INTRODUCTION

Since its discovery by Weedman et al. (1982), the $z = 2.15$ double quasar Q2345+007 A and B has been the subject of much controversy regarding whether or not it is gravitationally lensed. Although the two component images have remarkably similar redshifts, $\Delta v = 44 \pm 40 \text{ km s}^{-1}$ (Steidel & Sargent 1990, hereafter SS), the image separation of $7''.3$, largest among all known lens candidates, requires a very massive lensing system for which no evidence is apparent in deep broadband images by Tyson et al. (1986, hereafter TSWF).

Recently, some modest but statistically significant differences in the emission line spectra of Q2345+007 A and B have been found by SS. Although this seems to favor the binary (unlensed) quasar hypothesis, lensing time delays and intrinsic line variability might also explain the findings of SS, as we will show below.

High-resolution imaging studies of Q2345+007 have given various results. Nieto et al. (1988) detected a small ($0''.36$) splitting in image B, roughly parallel to the line connecting the two images. Weir & Djorgovski (1991, hereafter WD) also found a $\sim 0''.4$ extension (deviation from sphericity) of image B, but with the long axis in the orthogonal direction. The two groups may be in better agreement than it sounds, since Nieto et al. (1988) found a distortion of their outer (low) flux contours in the same direction as WD. The observed *splitting* was only in the innermost structure (high-flux contours) where Nieto et al. (1988) might have had better resolution. Both groups put strong limits ($\leq 0''.2$) on the splitting of the bright image (the luminosity ratio A:B is about 4:1). The observed splitting/extension, if verified, is probably most readily interpreted as evidence for lensing (Turner 1989), especially if the direction of splitting is radial as found by Nieto et al. (1988). If the image B splitting is really tangential, this cannot be due to a simple elliptical lensing potential, which produces tangentially split *bright* images only (Narayan, Blandford, & Nityananda 1984; Blandford & Kochanek 1987a). However, more complex lens configurations involving one or more galactic lenses augmented by a cluster potential might produce this image pattern (Turner, Ostriker, & Gott 1984, hereafter TOG; Nieto et al. 1988). An interesting alternative suggestion is that the lensing

is done by *two* dark galactic halos along the line of sight; this has non-negligible probability of occurring in the CDM cosmogony (Subramanian, Rees, & Chitre 1987). Finally, the image structure might also be due to a galaxy near (or surrounding) one component of a binary (unlensed) quasar (WD; see also Blandford & Kochanek 1987b). No firm conclusions can be made on the basis of these image studies.

As emphasized by SS, the question of whether or not Q2345+007 is lensed has significant implications for the “Ly α clouds,” the putative intergalactic gas concentrations observed in abundance via high- z quasar absorption line “forests.” High-resolution spectroscopy of Q2345+007A&B by Foltz et al. (1984, hereafter FWRC) revealed the presence of many common Ly α absorption lines, and some which were not common, in the two image spectra. This gives a rough measure of the cloud sizes, namely, that they are comparable to the average separation of the ray paths of the two images, which FWRC found to be $2\text{--}15 h_0^{-1}$ kpc, assuming the quasar is lensed. If the quasar is binary, as favored by SS, the ray paths at the Ly α forest are more widely separated by a factor of ~ 10 on average, which implies an upward revision in the size of the clouds by this factor.

In this Letter (§ 2) we will show that the narrow absorption line spectra themselves give evidence in favor of the lensing hypothesis. In § 3, we review the observational evidence, finding that it suggests the existence of a low-luminosity object of $10^{13} M_{\odot}$ contained within a volume of lateral extent $\sim 40 h_0^{-1}$ kpc.

2. EVIDENCE FROM THE LYMAN-ALPHA FOREST

If Q2345+007 is lensed, the basic geometry of the ray paths is illustrated in Figure 1. In this configuration, it is evident that Ly α absorption lines in the two image spectra should be strongly correlated at the high- z end of the spectrum [close to $z = z_0$ where the proper separation of raypaths $S(z) \rightarrow 0$], becoming less correlated with diminishing z . If the quasar is binary, on the other hand, the ray paths do not converge at z_0 , and less significant variation in the degree of narrow line correlation with z is expected.

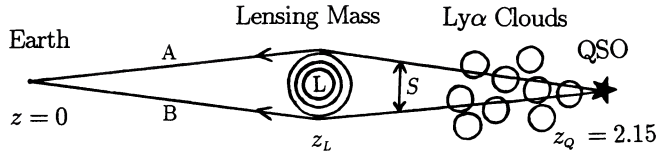


FIG. 1.—Lens geometry (schematic)

A careful examination of the FWRC spectral data lends support to the lensing hypothesis.¹ A subset of the FWRC line-list is given in Table 1. This includes only the strongest lines: $W \geq 0.50 \text{ \AA}$ (rest frame). Such lines are detected with greater than 4.5σ confidence even in the most noisy part of the spectrum (see Fig. 2 of FWRC). Since the 0.50 \AA counting threshold lies well above the noise limit, this line-list is complete: its membership is insignificantly affected by the trend of S/N with redshift.

Ray path separations $S(z)$ for both lensed and unlensed cases can be calculated by standard formulae (e.g., TOG; McGill 1990), and are listed in Table 1 at the redshifts of the lines.² In the range $2.11 > z > 1.86$ where $\text{Ly}\alpha$ lines are observed, $S(z)$ varies very little (only $\sim 3\%$) if the quasar is binary. This contrasts sharply with the lensed case, for which $S(z)$ varies from ~ 1 to $10 h_0^{-1} \text{ kpc}$ over the same range (i.e., 90% variation). The change in the cosmological scale parameter is only $3.11/2.86 = 1.1$ over the relevant range, so it is unlikely that the $\text{Ly}\alpha$ clouds evolve significantly. For example, if the clouds are expanding freely but approximately isothermally (due to photoionization heating) from a dense state at significantly higher redshift (Bond, Szalay, & Silk 1988), the cloud radii change by a factor of 1.15 ($q_0 = 0.5$) or 1.10 ($q_0 = 0$). Hence if the quasar is binary, the degree of narrow line correlation should change very little over the narrow z -range in which the $\text{Ly}\alpha$ forest is observed.

Table 1 shows a remarkable pattern: all observed “misses” (lines which have no observed match) occur at the low- z edge

¹ This was appreciated by FWRC, who said: “Our subjective judgement is that these additional observations very strongly support the view that 2345A, B is a gravitationally split image...”

² The $S(z)$ values in Table 1 are for lens redshift $z_L = 1.49$, a likely value based on heavy-element line observations (see § 3). However, the qualitative behavior of $S(z)$ which concerns us here, namely its variation by a large factor across the $\text{Ly}\alpha$ forest, is independent of z_L .

of the spectrum. This is the most probable configuration for a lens.

To study the implications of this pattern, imagine first that Q2345+007 is binary. The observed configuration (“misses” at line positions 1 and 2) is one of 21 possible configurations of two misses among seven different line locations. Since all configurations are equally likely in the binary model (to within an excellent approximation), the probability for the observed configuration occurring is $P_{\text{bnr}} = 1/21 = 0.048$.

If the quasar is lensed, the probability for the observed configuration is larger. To calculate how much larger, we need a model of the $\text{Ly}\alpha$ cloud population. The simplest plausible model is a population of uniform radius (R), homogeneous spherical clouds. In this case the probability Φ for a line-of-sight ray path to miss a cloud at a distance S away from a ray path that “hits” depends only on the ratio $y \equiv S/2R$, and is given by (McGill 1990; Duncan & Bajtlik 1991, hereafter DB):

$$\Phi = 1 - \frac{2}{\pi} [\cos^{-1} y - y(1 - y^2)^{1/2}] . \quad (1)$$

Assuming some value R , we can calculate Φ for each of the seven spectral lines in Table 1. For $q_0 = 0.5$ we take $R = (9.8 \pm 4.8) h_0^{-1} \text{ kpc}$, which is the best fit found by DB to all of the FWRC data (see Fig. 2). Then using the seven Φ -values we calculate the probability for a particular overall configuration, namely “missing” in the first two line positions (described by Φ_1 and Φ_2 , which are the largest Φ -values) and “hitting” in the other five, given that there are two misses overall. This lensing model probability for the observed configuration is just

$$P_{\text{lens}} = \frac{\Phi_1 \Phi_2}{P_2} \prod_{i=3}^7 (1 - \Phi_i) , \quad (2)$$

where P_2 is the sum over the probabilities for *all* configurations with two misses. We normalize to two misses since in calculating P_{bnr} we have assumed precisely two misses out of seven.

Under the usual Bayesian hypothesis of equal a priori probabilities, the likelihood ratio for lensing is $\mathcal{P}_L \equiv P_{\text{lens}}/P_{\text{bnr}}$. As shown in Table 2, $\mathcal{P}_L = 4.3$ for the most favored value of R , but it varies across the range of plausible R -values, with a chance that \mathcal{P}_L is as small as 3.4.³ The lensing likelihood is somewhat

³ The lensing likelihood drops off only gradually at higher R . For example, $\mathcal{P}_L = 3.0$ at $R = 21 h_0^{-1} \text{ kpc}$.

TABLE 1
ABSORPTION LINE DATA FOR Q2345+007A, B

LINE NUMBER	z	W_A^a	W_B^a	LENSED $S(z)^b$		UNLENSED $S(z)^b$	
				$q_0 = 0.5$	$q_0 = 0$	$q_0 = 0.5$	$q_0 = 0$
1.....	1.864	0.53	<0.43	10.6	15.5	30.3	46.7
2.....	1.873	<0.21	0.52	10.2	15.0	30.3	46.7
3.....	1.950	0.56	0.53	7.0	10.4	30.1	47.0
4.....	1.968	0.55	0.72	6.3	9.4	30.0	47.1
5.....	1.983	0.50	0.73	5.8	8.5	30.0	47.2
6.....	1.985	0.57	0.90	5.7	8.4	30.0	47.2
7.....	2.113	0.89	0.74	1.2	1.8	29.6	47.5

^a Observed rest-frame equivalent widths in \AA . This line-list includes only the strongest lines detected by FWRC: $W \geq 0.50 \text{ \AA}$. Where no line was detected, “<” indicates the 3σ upper bound.

^b Proper separation of ray paths at the location of the cloud, S , given in units $h_0^{-1} \text{ kpc}$, where $h_0 \equiv H_0/100 \text{ km s}^{-1} \text{ Mpc}^{-1}$. We assume a lensing mass redshift $z_L = 1.49$. Cosmological deceleration parameters q_0 used in calculating S are indicated above the columns.

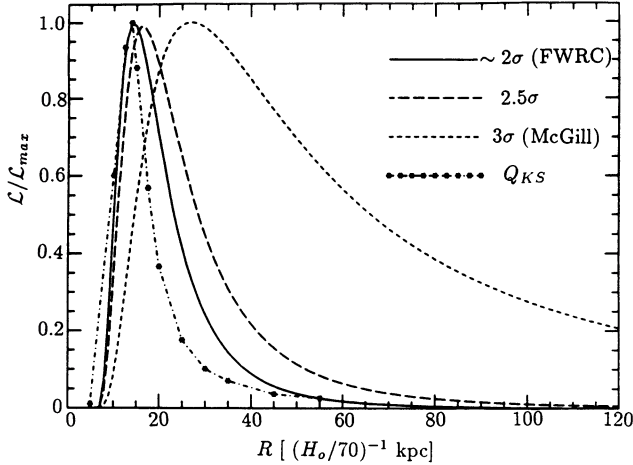


FIG. 2.—Statistical bounds on Ly α cloud radii R at $z \approx 2$ for a homogeneous, spherical cloud population, based on the data of FWRC and assuming that Q2345+007 is lensed. This figure is for $q_0 = 0.5$, $z_L = 1.49$. The short-dashed curve shows the bounds found by McGill (1990), using only the subset of the FWRC data in which line detections and nondetections were made with 3σ confidence. This (short-dashed) curve is a simple likelihood function for “hits” and “misses” based on eq. (1) of the text (see McGill 1990 for more details); the analysis does not use measured values of W . The long-dashed line shows the same analysis for the 2.5σ subset of the FWRC data; and the solid line is for all the lines listed by FWRC (roughly 2σ). Clearly as more data are used, stronger bounds on the cloud sizes are found, although these curves are not reliable beyond their respective confidence limits.

The “asterisk-dashed” line shows the Kolmogorov-Smirnov probability function Q_{KS} for the cloud radii as calculated by Duncan & Bajtlik (1991). This analysis takes into account all measurements of W and their statistical uncertainties, as well as all statistical bounds for “misses.” In this figure, Q_{KS} has been renormalized to unity at its maximum value to allow a rough comparison with the (similarly normalized) likelihood function; the real maximum value is $\max(Q_{KS}) = 0.90$, where $1 - Q_{KS}$ is the statistical confidence with which the model can be rejected.

In this figure only, the cloud radii scale as $[H_0/70 \text{ km s}^{-1} \text{ Mpc}^{-1}]^{-1}$; elsewhere scalings in terms of $H_0 = 100$ are used. The author thanks Stanislaw Bajtlik for help with the calculations shown here.

larger (5.3 to 1) if we assume $q_0 = 0$ rather than $q_0 = 0.5$. Note that all dependence on H_0 drops out of the analysis.

Technically speaking, what we are calling a “miss” is actually a nondetection with a certain statistical confidence (a certain statistical bound on W). Using the formulae of DB, one can calculate how \mathcal{P}_L changes if we include the possibility that the “misses” are actually hits to the fringes of clouds, where the ray paths intercept low N . This was done for one case ($q_0 = 0.5$, $R = 9.8h_0^{-1}$ kpc); \mathcal{P}_L went down by only 0.8%, not changing the quoted results. If the 3σ bounds on nondetections were not so stringent, this would be an important part of the analysis, however.

We have also done the analysis using an alternative one-parameter model of the Ly α cloud population—a model with uniform neutral hydrogen density n rather than uniform size R . This is appropriate for pressure-confined clouds of size less than the “crossover radius,” R_x (Duncan, Vishniac, & Ostriker 1991). The probability for a miss, Φ , then depends only on the parameter $x \equiv nS/N$. The functional form of Φ is given by DB. Note that in this model we need to convert equivalent widths W to column densities N ; we assumed $b = 25 + 14 (\log N - 14)$, where b is the velocity width in km s^{-1} . This is a reasonable fit of the line profile data of Pettini et al. (1990).⁴

TABLE 2
STATISTICAL TESTS FOR LENSING

CLOUD MODEL PARAMETERS ^a						
$R(h_0^{-1} \text{ kpc})$	$n_0(h_0^{-1} \text{ cm}^{-3})$	q_0	P_{lens}^b	$P_{\text{lens}}[\text{next}]^c$	P_{bnr}^d	\mathcal{P}_L^e
5.4	...	0.5	0.85	0.042	0.048	18.
9.8*	...	0.5	0.204	0.095	0.048	4.3
14.9	...	0.5	0.16	0.090	0.048	3.4
14.0*	...	0	0.253	0.117	0.048	5.3
...	2.4×10^{-9}	0.5	0.36	0.11	0.081	4.4
...	5.3×10^{-9} *	0.5	0.33	0.11	0.081	4.1
...	1.16×10^{-8}	0.5	0.32	0.11	0.081	4.0
...	3.35×10^{-10} *	0	0.33	0.11	0.073	4.5

^a Two different models for the Ly α cloud population are used: uniform radius (R) clouds (top four rows of table) and uniform neutral hydrogen density (n_0) clouds (bottom four rows). Asterisks (*) indicate values of the model parameters which give the best fit to all of the FWRC data (DB); these values are most reliable. The larger and smaller values of the model parameters, given in the $q_0 = 0.5$ cases, span the 1σ uncertainty range.

^b Given that seven lines are present of which two are misses, this is the probability for the observed configuration to occur (the two misses at the lowest z positions) assuming that the quasar is lensed.

^c Probability for the next most likely configuration, in which one of the misses moves to a higher z position, assuming that the quasar is lensed.

^d Probability for the observed configuration to occur if the quasar is binary, i.e., NOT lensed.

^e Likelihood ratio for gravitational lensing, $\mathcal{P}_L \equiv P_{\text{lens}}/P_{\text{bnr}}$.

Results for the uniform- n model are given in the last four rows of Table 2. Note that P_{bnr} is not simply $1/21$ because Φ now depends on N (or W) as well as S .

Our calculations of \mathcal{P}_L assume $z_L = 1.49$, which is a plausible value (§ 3). However, the lensing likelihood does not vary strongly with z_L . This is because the model parameters R and n are themselves based on fits to the FWRC data; there exist at present no independent data on Ly α cloud sizes. The model parameters thus scale with z_L in such a way that the Φ functions are only weakly dependent on z_L , a fact that we have explicitly verified. If there were independent data on the cloud sizes and densities, then \mathcal{P}_L would depend on z_L .

We conclude that in either model, the likelihood for gravitational lensing is roughly 4 to 1.⁵ Since any realistic model of the Ly α cloud population is likely to include both size and density variations, the above two models span the range of plausible homogeneous cloud models. Furthermore, there is no reason to expect very different results for this test even with more complex cloud models (e.g., Ikeuchi, Murakami, & Rees 1988),

3. THE DARK LENS

The main evidence for lensing in Q2345+007 is: (1) the lenslike pattern of Ly α absorption features (analyzed above); and (2) the small velocity difference of the emission features

⁴ Carswell et al. (1991) find many higher b lines, in disagreement with Pettini et al. (1990). Data on Q2345+007 of high enough quality to allow profile fitting would significantly increase the reliability of the uniform- n model tests.

⁵ If one adopts a counting threshold that is slightly less restrictive than $W > 0.50 \text{ \AA}$, the nominal lensing likelihood goes up significantly. But when the W -threshold is lowered, at some point there is danger of the test being biased by the general S/N trend in the spectra. The counting criterion we have taken is very conservative.

found by SS: $\Delta v = 44 \pm 40 \text{ km s}^{-1}$. This Δv is smaller than most galaxy group or cluster velocity dispersions. If Q2345+007 consists of two quasars in a cluster with velocity dispersion σ_v , you would see Δv this small only a fraction ~ 0.06 ($\sigma_v/700 \text{ km s}^{-1}$) of the time. Although not conclusive, this evidence is interesting enough to warrant further investigation.

Recall that SS detected significant differences in the emission line spectra of A and B, a circumstance that is most easily explained if the quasar is binary. However, quasar variability studies (e.g., O'Brien et al. 1988; Sitko 1990) indicate that it is also plausible that the C III/Mg II line ratio and C III/continuum ratio would vary by a factor 1.43, as found by SS, over a period $\sim 3\text{--}5$ yr, the lens time delay. There is evidence for variability of the magnitude difference $m_A - m_B$ during the past 8 yr (Sol et al. 1984; WD); this continuum variability can drive changes in the broad-line region (Clavel et al. 1991; Korantkar & Gaskell 1991). Present photometry data are too sparsely sampled in time to determine if the spectral discrepancy is caused this way. Microlensing could produce spectral differences as well (Filippenko 1989).

Assuming that the quasar is lensed, possible clues concerning the lensing object can be found in heavy element absorption lines. Many metal lines have been detected in the spectrum of both images at redshift $z = 1.491$ (FWRC; TSWF; SS). There also exists a second C IV doublet in image B at shifted frequency: $\Delta V(\text{C IV}) = 1060 \pm 60 \text{ km s}^{-1}$, a velocity difference comparable to σ_v for a rich cluster. No other metal-line systems were found in either image down to $z \sim 0.8$ (SS).

If these absorptions are associated with a lensing cluster at $z_L = 1.49$, the critical surface density for lensing is (TOG)

$$\Sigma_c = \frac{c^2 D_q}{4\pi G D_{qL} D_L} = 2.0 - 1.3 h_0 \text{ gm cm}^{-2}, \quad (3)$$

where the two quoted values are for $q_0 = 0.5$ and 0. With velocity dispersion $\sigma_v \sim \Delta V(\text{C IV})$, the core radius of this object, idealized as isothermal, would be

$$r_c = \frac{9\sigma_v^2}{2\pi\Sigma(0)} = 36 - 53 h_0^{-1} \left(\frac{\sigma_v}{1000} \right)^2 \left[\frac{\Sigma(0)}{\Sigma_c} \right]^{-1} \text{ kpc}, \quad (4)$$

which corresponds to an angular size $8''.5$ (independent of q_0), comparable to the image spacing.

A concentration of mass $M \sim \pi(40 \text{ kpc})^2 \Sigma_c \sim 10^{13} M_\odot$ seems to be required, for which no obvious evidence was found in deep broad-band images (TSWF). As shown by TSWF, an

Abell Class 4 cluster [$\sigma_v \sim \Delta V(\text{C IV})$] extrapolated to $z = 1.5$ with plausible evolution would have easily been detected; any cluster which is actually present at $z = 1.5$ is comparatively underluminous by a factor of ~ 10 or more.

We now suggest several observational approaches to studying this system.

3.1. Spectroscopy of Other Quasar Pairs: the Sizes of Ly α Clouds

It would be instructive to measure the Ly α forest spectrum of a confirmed $z > 2$ binary quasar with angular separation $\sim 10''$. If Q2345+007 is binary, the diameters of the Ly α clouds at $z \approx 2$ are $120 \pm 42 h_0^{-1} \text{ kpc}$ [$q_0 = 0.5$], or $182 \pm 64 h_0^{-1} \text{ kpc}$ [$q_0 = 0$] (DB). Binary quasar spectra could determine whether the clouds are really this large, and hence if Q2345+007 is lensed (Crofts & Duncan 1991).

3.2. Deep Imaging

More deep searches should be made. In particular, since the 4000 Å break in the spectra of normal galaxies is redshifted to $1 \mu\text{m}$ (the red limit of the *I*-band) at $z = 1.5$, a more sensitive study of the candidate lensing cluster could be done by going farther in the infrared than was explored by TWRC (E. Turner 1991, private communication). One might also detect non-luminous matter in Q2345+007 via the alignment of many faint, blue, gravitationally distorted background field galaxies (Tyson, Valdes, & Wenk 1990).

3.3. Redshifted 21 cm Emission

For a lensing object at $z_L = 1.49$, the baryon column density is $N_b = 10^{23} (\Sigma/\Sigma_c) (Y_b/0.1) \text{ cm}^{-2}$, where Y_b is baryon mass-fraction, scaled in terms of a value [0.1] consistent with nucleosynthesis constraints in an $\Omega = 1$ universe. Since the cluster is underluminous, much of this column density might be in gaseous form. It is not clear how much is in neutral hydrogen, but even a small fraction is potentially detectable in 21 cm emission redshifted to $z = 1.491$ (570.2 MHz) (Narasimha & Chitre 1989; Duncan, Higdon, & Fischer 1991).

I thank S. Bajtlik, R. Blandford, S. Phinney, E. Turner, T. Tyson, and E. Vishniac for helpful discussions. I especially thank S. Bajtlik for allowing me to quote in advance some results of our collaborative study of Ly α cloud sizes. This research was supported by the Texas Advanced Research Program, and by an NSF grant for theoretical cosmology at the University of Texas.

REFERENCES

- Blandford, R. D., & Kochanek, C. S. 1987a, *ApJ*, 321, 658
 ———. 1987b, in *Dark Matter in the Universe: Proceedings of the Fourth Jerusalem Winter School for Theoretical Physics*, ed. J. Bahcall et al. (Singapore: World Scientific), 133
 Bond, J. R., Szalay, A. S., & Silk, J. 1988, *ApJ*, 324, 627
 Carswell, R. F., Lanzetta, K. M., Parnell, H. C., & Webb, J. K. 1991, *ApJ*, 371, 36
 Clavel, J., et al. 1991, *ApJ*, 366, 64
 Crofts, A., & Duncan, R. 1991, observing proposal
 Duncan, R. C., & Bajtlik, S. 1991, in preparation (DB)
 Duncan, R., Higdon, J., & Fischer, R. 1991, observing proposal
 Duncan, R. C., Vishniac, E. T., & Ostriker, J. P. 1991, *ApJ*, 368, L1
 Filippenko, A. V. 1989, *ApJ*, 338, L49
 Foltz, C. B., Weymann, R. J., Roser, H. J., & Chaffee, F. H. 1984, *ApJ*, 281, L1 (FWRC)
 Ikeuchi, S., Murakami, I., & Rees, M. J. 1988, *MNRAS*, 236, 21p
 Korantkar, A. P., & Gaskell, C. M. 1991, *ApJ*, 370, L61
 McGill, C. 1990, *MNRAS*, 242, 544
 Narasimha, D. & Chitre, S. M. 1989, *AJ*, 97, 327
 Narayan, R., Blandford, R., & Nityananda, R. 1984, *Nature*, 310, 112
 Nieto, J. L., Roques, S., Liebaria, A., Vanderriest, Ch., Lelièvre, G., di Serego Alighieri, S., Macchetto, F. D., & Perryman, M. A. C. 1988, *ApJ*, 325, 644
 O'Brien, P. T., Gondhalekar, P. M., & Wilson, R. 1988, *MNRAS*, 233, 845
 Pettini, M., Hunstead, R. W., Smith, L. J., & Mar, D. P. 1990, *MNRAS*, 246, 545
 Sitko, M. L. 1990, *ApJS*, 72, 777
 Sol, H., Vanderriest, C., Lelièvre, G., Pedersen, H., & Schneider, J. 1984, *A&A*, 132, 105
 Steidel, C. C., & Sargent, W. L. W. 1990, *AJ*, 99, 1693 (SS)
 Subramanian, K., Rees, M. J., & Chitre, S. M. 1987, *MNRAS*, 224, 283
 Turner, E. L. 1989, in *Gravitational Lenses*, ed. J. M. Moran et al. (Berlin: Springer), 71
 Turner, E. L., Ostriker, J. P., & Gott, J. R. 1984, *ApJ*, 284, 1 (TOG)
 Tyson, J. A., Seitzer, P., Weymann, R. J., & Foltz, C. 1986, *AJ*, 91, 1274 (TSWF)
 Tyson, J. A., Valdes, F., & Wenk, R. A. 1990, *ApJ*, 349, L1
 Weedman, D., Weymann, R. J., Green, R. F., & Heckman, J. M. 1982, *ApJ*, 255, L5
 Weir, N., & Djorgovski, S. 1991, *AJ*, 101, 66 (WD)